ADDIS ABABA UNIVERSITY
SCHOOL OF GRADUATE STUDIES
DEPARTMENT OF CHEMISTRY

THEORETICAL STUDIES OF NATURALLY OCCURING HOMOISOFLAVONOIDS

GRADUATE PROJECT (Chem.774)

By

MERESSA ABRHA

ADVISOR: Dr. AHMED MUSTEFA

A Graduate Project

Submitted to

the School of Graduate Studies of Addis Ababa University in partial Fulfillment of the Requirements for the Degree of Master of Science in Chemistry

JULY, 2009

ADDIS ABABA UNIVERSITY
SCHOOL OF GRADUATE STUDIES
DEPARTMENT OF CHEMISTRY

THEORETICAL STUDIES OF NATURALLY OCCURING HOMOISOFLAVONOIDS

MERESSA ABRHA

Approved by the Examination board Signature

Dr. Ahmed Mustefa _____

Advisor

Dr. Mesfin Redi _____

Examiner

Dr. Teketel Yohanes _____

Examiner

Declaration

I, the undersigned, declare that this is my original work and has not been submitted for a degree in any other university and all sources of material used for the project have been duly acknowledged.

Name: Meressa Abrha

Signature:_____

This project has been submitted for examination with my approval as university advisor.

Name: Dr. Ahmed Mustefa

Signature: _____

Place and date of submission:

School of Graduate Studies

Addis Ababa University

July, 2009

Acknowledgements

I wish to express my sincere appreciation to my advisor Dr. Ahmed Mustefa for his guidance, encouragement, conception and creating the most favorable situation possible to do the project work.

I extend my real appreciation and thanks to Professor Wendimagegn Mammo for his conception and encouragement of this problem.

I also wish to express my sincere gratitude to Madawalabu University (MWU) for their sponsorship or financial support.

Finally, I would like to express my thanks to my relatives and best friends for their motivation and encouragement during the course of this work.

TABLE OF CONTENTS

List of tables

List of figures

Page

Abbreviations

anis = anisotropic

B3LYP = Becke three-parameter Lee-Yang-Parr correlation functional

CNDO = Complete Neglect of Differential Overlap

DFT = Density Functional Theory

GIAO = Gauge Independent/Invariance Atomic Orbital

GTO = Gaussian Type Orbitals

HF = Hartree-Fock

HOMO = Highest Occupied Molecular Orbital

IR = Infrared

INDO = Intermediate Neglect of Differential Overlap

iso = isotropic

LCAO = Linear Combination of Atomic Orbitals

LUMO = Lowest Unoccupied Molecular Orbital

NMR = Nuclear Magnetic Resonance

ppm = parts per million

ref = reference

SD = Slater Determinant

SCF = Self-Consistent Field

STO = Slater Type Orbital

T.M = Transition Moment

TMS = Tetramethylsilane

UV = Ultraviolet

xc = exchange-correlation

ZDO = Zero Differential Overlap

Abstract

Nowadays molecular modelling becomes an alternative way for sophisticated and costly experimental techniques. In this project the structures of five naturally occurring homoisoflavonoids namely; 5, 7-dihydroxy-6-methoxy-3-(4'-hydroxybenzyl) chroman-4-one (**A**), 7-hydroxy-3-(4'-hydroxybenzyl) flavone (**B**), (E)-7-hydroxy-3-(4'-methoxybenzylidene) chroman-4-one (**C**), Brazilin (7, 11b-dihydrobenz[b]indeno [1, 2-d] pyran-3, 6a, 9, 10, (6H)-tetrol) (**D**) and 5, 7-hydroxy-3', 4'-dimethoxyspiro {2H-1-benzopyran-3-bicyclo [4.2.0] octa [1'.3'.5']-trien}-4-one (**E**) are determined by geometry optimization using Density Functional Theory. Comparison of optimized structural parameters like bond lengths, bond angles and torsional (dihedral) angles are extracted. Computation of molecular properties such as NMR shielding tensors (^{1}H and ^{13}C chemical shifts with respect to TMS), infrared harmonic vibrational frequency (scaled with 0.9614) and UV-absorption transitions of these natural homoisoflavonoids are reported here. Calculated results are found to be in good agreement with the experimentally observed values. Though IR absorption frequency spectra and UV absorption spectra were done in gas-phase, the obtained results are in good agreement with the experimental values.

1. Introduction

The quantitative nature of scientific theories allows them to be tested by experiment. This testing is the means by which the applicable range of a theory is elucidated. Hypothesis (an educated guess or logical conclusion from known facts) is the first step in the scientific method [1]. If the hypothesis is found to be consistent with known facts, it is called a theory and then leads to a scientific law. Computational chemistry is generally used when a mathematical method is sufficiently well developed and automated for implementation on a computer. Almost every aspect of chemistry has been described in a qualitative or approximately quantitative computational scheme. Energy is one of the most useful concepts in computational science in which all computational chemistry techniques define energy such that the system with the lowest energy is the most stable. Thus, finding the most stable structure of a molecule corresponds to its practical importance on chemical researches.

1.1 Computational chemistry

Computational chemistry is a subfield of theoretical chemistry that uses efficient computer programs to assist in solving chemical problems like calculating the structures and properties of molecules and thereby the results are normally complement with the information obtained by chemical experiments. By virtue of the great flexibility and power of electronic computers, basic principles of classical and quantum mechanics are now implemented in a form which can handle the many-body problems associated with the structure and behavior of complex molecular systems. Molecular mechanics which uses the laws of classical physics (Newton laws) and electronic structure methods that uses the laws of quantum mechanics are the two broad areas within computational chemistry.

The programs used in computational chemistry are based on many different quantum-chemical methods that solve the molecular Schrödinger equation associated with the molecular Hamiltonian (the energy of the electrons and nuclei in a molecule). Thus, the

ultimate goal of most quantum chemical approaches is the approximate solution of the time-independent, non-relativistic Schrödinger equation which is given by

$$\hat{\mathrm{H}}\Psi_i(r,R) = \mathrm{E}_i\Psi_i(r,R) \tag{1.1}$$

where r the coordinates of the electrons and R the coordinates of the nuclei. $\hat{\mathrm{H}}$ is the Hamilton operator for a molecular system containing of M nuclei and N electrons in the absence of magnetic or electric fields [2].

$$\hat{\mathrm{H}} = -\frac{1}{2}\sum_{i=1}^{N}\nabla_i^2 - \frac{1}{2}\sum_{A=1}^{M}\frac{1}{M_A}\nabla_A^2 - \sum_{i=1}^{N}\sum_{A=1}^{M}\frac{Z_A}{r_{iA}} + \sum_{i=1}^{N}\sum_{j>i}^{N}\frac{1}{r_{ij}} + \sum_{A=1}^{M}\sum_{B>A}^{M}\frac{Z_A Z_B}{R_{AB}} \tag{1.2}$$

i and j denotes the N electrons in the system while A and B run over the M nuclei. E_i is the numerical value of energy of the state described by wave function, Ψ_i and M_A is the mass of nucleus A. The first two terms describe the kinetic energy of the electrons and nuclei respectively. The remaining three terms define the potential part of the Hamiltonian, of which, the third term describes the electron-nuclei attraction and the fourth and fifth terms represents the electron-electron and nuclei-nuclei repulsions respectively. It is noted that the mass of nuclei is much greater than that of electrons and thereby electrons move much faster than the nuclei. Hence, the motion of the nuclei and electrons can be separated. This is known as the Born-Oppenheimer Approximation, the complete Hamiltonian given in equation 1.2 is then reduced to so called the electronic Hamiltonian, $\hat{\mathrm{H}}_e$:

$$\hat{\mathrm{H}}_e = -\frac{1}{N}\sum_{i=1}^{N}\nabla_i^2 - \sum_{i=1}^{N}\sum_{A=1}^{M}\frac{Z_A}{r_{iA}} + \sum_{i=1}^{N}\sum_{j>i}^{N}\frac{1}{r_{ij}} = \widehat{\mathrm{T}}_e + \hat{V}_{Ne} + \hat{V}_{ee} \tag{1.3}$$

where $\hat{\mathrm{T}}$ and $\hat{V}$ symbols represent for kinetic energy and potential energy respectively.

Indeed a very important consequence of the Born-Oppenheimer approximation is the assumption that the potential energy surface (or the effective force constants) of a molecule is unchanged upon isotopic substitution. The electronic wavefunction depends parametrically on nuclear coordinates (position of nuclei) but not on their momenta [3]. A physical interpretation can only be associated with the square of the wavefunction in that $\left|\Psi(\vec{\chi}_1,\vec{\chi}_2,\ldots\vec{\chi}_N)\right|^2 d\vec{\chi}_1 d\vec{\chi}_2 \ldots d\vec{\chi}_N$ represents the probability that electrons 1, 2,…,N are found simultaneously in volume elements $d\vec{\chi}_1 d\vec{\chi}_2 \ldots d\vec{\chi}_N$. Hence, the probability of finding N electrons anywhere in space must be exactly unity i.e. the wave function satisfying this

condition is called normalized. The Born-Oppenheimer Approximation and the variational principle assumptions are important in solving the time-independent Schrödinger equation. The variational principle [4] states that the energy expectation value, E_{trial} of the Hamiltonian operator $\hat{H}$ from any guessed Ψ_{trial} is always greater than (the upper bound) or equal to the true ground-state energy, E_0, of the system.

$$E_{trial} = \frac{\langle \Psi_{trial} \left| \hat{H} \right| \Psi_{trial} \rangle}{\langle \Psi_{trial} \Psi_{trial} \rangle} \geq E_0 \qquad (1.4)$$

The equality occurs only when the trial wavefunction is the true ground-state wavefunction of the system.

1.1.1 The *ab initio* (Hartree-Fock) method

Ab initio (Latin from the scratch) methods use equations that are being derived directly from theoretical principles, with no inclusion of experimental data. The most intermediate contrast with semi-empirical methods is the fact that all integrals are evaluated from the scratch [5]. It is assumed that electronic wavefunctions are not affected by nuclear motion (Born-Oppenheimer Approximation). Thus, each electronic structure calculation is performed for a fixed nuclear configuration. The electronic structure of molecules can only be treated by quantum mechanics, since the electrons are very quickly moving particles.

In *ab initio* method, computational time varies approximately as the fourth power of the number of basis functions. The Slater-Type Orbital, STO-3G, is taken as a minimum basis set because it uses only the number of orbitals required to accommodate the number of electrons for the atom in question. The simplest type of *ab initio* electronic structure calculation is the Hartree-Fock (HF) scheme which is an extension of molecular orbital theory and thereby the correlated electron-electron repulsion is not specifically taken into account (only its average effect is included in the calculation). Electrons are fermions with half-integral spin and the wavefunction is antisymmetric with respect to interchange of the spatial and spin coordinates of any two electrons.

$$\Psi(\vec{\chi}_1, \vec{\chi}_2, \ldots \vec{\chi}_i, \vec{\chi}_j, \ldots \vec{\chi}_N) = -\Psi(\vec{\chi}_1, \vec{\chi}_2, \ldots \vec{\chi}_j, \vec{\chi}_i, \ldots \vec{\chi}_N) \tag{1.5}$$

The simplest antisymmetric function (which is a combination of molecular orbitals) is a determinant. The antisymmetry of wavefunction can be achieved by building it from Slater determinants which was first exploited by Slater (1929) and are used in a standard Hartree-Fock calculation [6]. The columns in a Slater determinant represents single electron wavefunctions (orbitals) while the electron coordinates are along the rows. The spin orbitals, ϕ (the product of the molecular orbital and a spin function) are orthonormal. Generally, for N electrons and N spin orbitals the Slater determinant, Ψ_{SD} is given as

$$\Psi_{SD} = \frac{1}{\sqrt{N!}} \begin{vmatrix} \phi_1(1) & \phi_2(1) & \cdots & \phi_N(1) \\ \phi_1(2) & \phi_2(2) & \cdots & \phi_N(2) \\ \vdots & \vdots & \ddots & \vdots \\ \phi_1(N) & \phi_2(N) & \cdots & \phi_N(N) \end{vmatrix} \tag{1.6}$$

where $(N!)^{-\frac{1}{2}}$ prefactor ensures that Ψ_{SD} fulfills the normalization condition. The Slater determinant is the exact wave function on N non-interacting particles moving in the field of the effective potential and thereby applies only to closed shell systems of non-degenerate point group symmetry; otherwise, the wave function consists of a linear combination of a few Slater determinants.

Fundamentally, all *ab initio* calculations start out at the Hartree-Fock Self-Consistence Field (HF-SCF) which involves an iterative process, in that, the orbitals are improved from cycle to cycle until the electronic energy reaches a constant minimum value and the orbitals no longer change with the mean field of other electrons in the molecule. In SCF theory, closed-shell systems are calculated using restricted Hartree-Fock, RHF theory while open-shell molecules (with unpaired electrons) use unrestricted Hartree-Fock, UHF formalism [7]. As the basis set size is increased, the energy and wave function tend towards a limit (the limit of an infinite basis set) called the Hartree-Fock limit. The wave function is formed from linear combinations of atomic orbitals or more often from linear combinations of basis functions. The Linear Combination of Atomic Orbitals (LCAO) involves finding the combination of atomic orbitals having proper symmetries that give the lowest (most

negative) electronic energy. The molecular orbital ϕ_i is given as a linear combination of N basis functions by

$$\phi_i = \sum_{\mu=1}^{N} C_{\mu i}\chi_\mu \tag{1.7}$$

where $C_{\mu i}$ is molecular orbital coefficient of the basis function χ_μ. Because of this approximation, most HF calculations give a computed energy greater than the Hartree Fock limit. The greater the number of basis functions the better the wavefunction, the lower the energy. The basis functions or basis sets can be either the Slater-Type Orbitals (STO) or Gaussian-Type Orbitals (GTO) which are expressed as follows.

$$\chi_{STO}(r) = Nx^l y^m z^n e^{-\zeta r} \text{ and } \chi_{GTO}(r) = Nx^l y^m z^n e^{-\alpha r^2} \tag{1.8}$$

N is the normalization factor, α and ζ are orbital exponents. r is the distance from the nucleus, x, y, z are Cartesian variables and l, m, n determine the order of the function such that $l + m + n = 0$ represents s-orbitals.

The approximate solution of the Hartree-Fock equations is not exact, because the true wavefunction is not a product of two orbitals, but is rather a complicated function of both variables simultaneously. The HF method suffers from the fact that it approximates the many electron problems as a one electron problem and implies that the each electron sees the other electrons as a mean-field. Most common methods to include electron correlation are Configuration Interaction (CI), Coupled Cluster (CC), Perturbation Theories (MPn), and Density Functional Theory (DFT)

1.1.2 Semi-empirical methods

Most current general-purpose semiempirical methods are based on MO theory and employ a minimal basis set; Slater Type Orbitals (not Gaussian) for the valence electrons and these methods describe only ground-states. Electron correlation is treated explicitly only if this is necessary for an appropriate zero-order description. The central assumption of Semi-empirical methods is the Zero Differential Overlap (ZDO) [8] approximation, which neglects all products of basis functions depending on the same electron coordinates when

located on different atoms. CNDO (Complete Neglect of Differential Overlap), INDO (Intermediate Neglect of Differential Overlap) [9] and NDDO (Neglect of Diatomic Differential Overlap) are some of the levels of integral approximation methods. Defining how many integrals are neglected and how the parameterization is done, defines these various semi-empirical methods. NDDO is the best of these approximations.

In Semi-empirical methods, all the three-and four-center electron integrals, which are the most numerous of the two-electron integrals are neglected. In order to compensate these approximations the remaining integrals are made in to parameters, and their values are assigned on the basis of calculations or experimental data. Semi-empirical methods attempt to speed up Hartree-Fock integrals by replacing some of the two-electron integrals and follow empirical methods where the two-electron part of the Hamiltonian is not explicitly included. The Hückel method for π-electron systems and Extended Hückel method for all valence electron systems are examples of Semi-empirical methods.

1.1.3 Density Functional Theory

Density Functional Theory (DFT) method is the most popular and versatile quantum mechanical method available in computational science to investigate the electronic structure of many-electron systems and the total energy is expressed interms of the total electronic density rather than the wavefunction. The electron density (square of the wave function) is the number of electrons per unit volume for a given state and only depends on three coordinates; independently of the number of electrons. While the complexity of a wavefunction increases with the number of electrons, the electron density has the same number of variables, independently of the system size. Hence, in DFT the ground-state electronic energy is determined completely by the electron density, ρ [10]. Although each different density yields different ground state energy, the functional connecting these two quantities is not known. The main goal of DFT is therefore to design functionals connecting the electron density with the energy. The energy functional may be divided in to three parts *viz* kinetic energy ($T[\rho]$), attraction between the nuclei and electrons ($E_{ne}[\rho]$), and electron-electron repulsion ($E_{ee}[\rho]$) since the nuclear-nuclear repulsion is constant in

the Born-Oppenheimer approximation. Following the work of Kohn and Sham, the approximate functionals employed by current DFT methods, the general energy, $\mathrm{E}_{DFT}[\rho]$ expression can be written as [11]

$$\mathrm{E}_{DFT}[\rho] = \mathrm{T}_s[\rho] + \mathrm{E}_{ne}[\rho] + J[\rho] + \mathrm{E}_{xc}[\rho] \tag{1.12}$$

where $\mathrm{E}_{xc}[\rho] = (\mathrm{T}[\rho] - \mathrm{T}_s[\rho]) + (\mathrm{E}_{ee}[\rho] - J[\rho])$ is the exchange-correlation term, of which, the first term refers to the kinetic correlation energy while the second part contains both exchange and potential correlation energy. $\mathrm{T}[\rho]$ is the total kinetic energy and $\mathrm{T}_s[\rho]$ kinetic energy calculated from a Slater determinant. $J[\rho]$ is the columbic electron repulsion term. The exchange-correlation potential V_{xc}, which is the functional derivative of energy, E_{xc} is given by

$$V_{xc} = \frac{\partial \mathrm{E}_{xc}}{\partial \rho} \tag{1.13}$$

The general Kohn-Sham equation is given by

$$\mathrm{H}\psi_i(r) = -\frac{1}{2}\nabla^2\psi_i(r) + V_{eff}(r)\psi_i(r) = \varepsilon\psi_i(r) \tag{1.14}$$

where $V_{eff}(r) = V_{ext}(r) + V_{HF}(r) + V_{xc}(r)$ for external, Hartree-Fock, and exchange-correlation potentials.

Density functional methods such as local, gradient corrected and hybrid forms have been developed for describing this exchange-correlation. The Local Density Approximation (LDA) is the basic assumption for almost all approximations currently used in DFT. It is assumed that the density locally can be treated as a uniform electron gas, or equivalently that the density is a slowly varying function. The simplest approximation for the exchange-correlation is given by

$$\mathrm{E}_{xc}^{LDA} = \int e_{xc}(\rho)\rho(r)\,dr \tag{1.15}$$

where $e_{xc}(\rho)$ is the exchange-correlation energy per particle of a uniform electron gas of density ρ.

The Gradient Corrected methods, some times called as non-local methods, treated as a non-uniform electron gas and thereby the exchange and correlation energies are dependent on both the electron density and derivatives of the density. The Hybrid methods are models which include exact exchange. In practice, self-consistent Kohn-Sham DFT calculations are performed in an iterative manner that is analogous to the SCF computation. Recently, Becke has formulated functionals which include a mixture of HF and DFT exchange along with DFT correlation which is called B3LYP (for Becke three-parameter Lee-Yang and Parr) functional and has the following form [12]

$$\mathrm{E}_{XC}^{B3LYP} = (1-a_0)\mathrm{E}_X^{LSDA} + a_0\mathrm{E}_X^{exact} + b_0\Delta\mathrm{E}_X^{B88} + \mathrm{E}_C^{LSDA} + c_0\Delta\mathrm{E}_C^{GGA} \qquad (1.16)$$

a_0, b_0 and c_0 are parameters determined by fitting to experimental data with values, a_0=0.20, b_0=0.72, and c_0=0.81 of which the parameter a_0 allows any admixture of the HF and LDA local exchange to be used.

Today, B3LYP is probably the most used density functional in chemistry, and the reason for the growing popularity of DFT in calculations of molecules. Unlike HF, DFT contains no approximations and in principle it is exact.

1.2 Geometry optimization

Geometry optimization (also called minimizations) begin at the molecular structure specified as its input and locate minima on the potential energy surface, thereby predicting equilibrium structures of molecular structures. It computes the energy and the gradient at that point [13]. The gradient, which is the first derivative of the energy with respect to the molecular coordinates, indicates the direction along the surface in which the energy decreases most rapidly from the current point as well as the steepness of that slope. Generally, at a minimum point, the first derivatives (gradient, g) with respect to χ_i of E are zero and the second derivative (Hessian, H_i) is positive:

$$g = \frac{\partial \mathrm{E}}{\partial \chi_i} = 0 \;; \quad \mathrm{H}_i = \frac{\partial^2 \mathrm{E}}{\partial \chi_i^{\,2}} > 0 \qquad (1.17)$$

Hessian matrix is the square matrix of second-order partial derivatives of a function that describes the local curvature of a function of many variables. It is noted that if all Hessian eigenvalues are positive a minimum value is found. Moreover, maximum value is obtained if all Hessian eigenvalues are negative, while the mixture of positive & negative eigenvalues results in so called saddle point. The stationary points found on the molecular potential energy hypersurfaces were characterized by numerical harmonic vibrational analysis. Optimized structures were confirmed to be a stationary point of minimum energy on potential energy surface by calculation of vibrational frequencies at the stated geometry. The absence of imaginary frequencies (negative eigenvalues of Hessian matrices) which correspond to real minima instead of being saddle points and a threshold of $<50cm^{-1}$ were used as a confirmation of the geometry's validity for further property calculations. Since real molecules are always in motion, in order to describe the structural analysis of a given molecule, a single molecule rigid structure (fixed geometry) is to be considered. This rigid structure is optimized so as to get the lowest energy (most stable) structure of the compound of interest. For energy and gradient computation, the Quasi-Newton algorithm is used. The Berny algorithm is one of the most efficient Quasi-Newton algorithms (which assume a quadratic potential surface) which internally build up a second derivative Hessian matrix.

1.3 Homoisoflavonoids

Traditional plants may represent new sources of anti-microbial with stable, biologically active components that can establish a scientific base for the use of plants in modern medicine. These can be extended for future investigation into the field of Pharmacology, Phytochemistry, Ethnobotany and other biological actions for drug discovery. Naturally occurring homoisoflavonoids are a very important class of secondary metabolites which possess a wide range of biological activities including antimicrobial, anti-mutagenic, anti-inflammatory, anti-diabetic and so on like properties [14]. That is why we are interested in studying the structural elucidation of homoisoflavonoids in this project. The term homoisoflavanone was considered inappropriate as these compounds are not derived from isoflavones by insertion of a one carbon unit; instead contain dihydropyrone rings [15].

Homoisoflavonoids may be classified in to the following five groups by considering their carbon frame work and biogenetic possibilities [16]. The general structural representations of the types of homoisoflavonoids are given in figure 1.

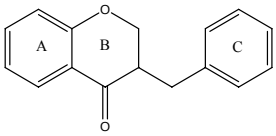

I. 3-benzyl chroman-4-ones

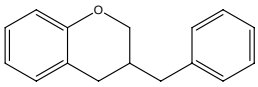

II. 3-benzylflavans

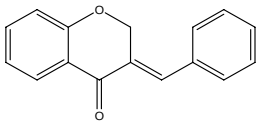

III. 3-benzylidene-4-chromanones

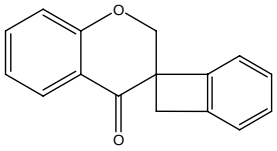

IV. Benzocyclobutene (scilliscillins)

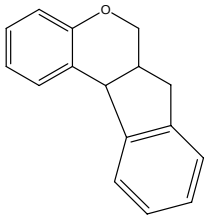

V. Rearranged homoisoflavonoids

Figure 1. General classification of homoisoflavonoids

The great majority of natural homoisoflavonoids are grouped under the 3-benzyl chroman-4-ones (homoisoflavanones) which are distributed in the Hyacynthaceae family and have been showed several activities [17]. Isoflavonoids are based on the 3-phenylchroman skeleton that is biogenetically derived by an aryl migration from a flavanone precursor. These have an important role in obese and insulin-resistant postmenopausal women. However, high-dose isoflavones affects on metabolic and inflammatory markers in healthy postmenopausal women.

1.4 Molecular properties

Molecular properties are expressed as the derivatives of the molecular energy with respect to applied perturbations or mixed derivatives like differentiating once with respect to an applied electric field and once with respect to nuclear displacements give the dipole derivative, whose square is the intensity of an IR transition. For example, the harmonic force constants are second derivatives of the energy with respect to displacement of the nuclei. Differentiating with respect to a magnetic field gives magnetic susceptibility or spin-spin coupling constants up on differentiating with respect to nuclear magnetic moments and so on.

Spectroscopy is the study of quantized interaction of energy (typically electromagnetic energy) with matter. The data that is obtained from spectroscopy is called a spectrum. A spectrum is a plot of the intensity of energy detected versus the wavelength (or mass or momentum or frequency, etc.) of the energy.

1.4.1 The NMR shielding tensors and chemical shifts

Nuclear magnetic resonance (NMR) spectroscopy is a valuable technique for obtaining chemical information as well as structure determination of large number of molecules including metabolites and proteins in solution [1, 3]. The atomic properties of the atomic nucleus form the basis of NMR spectroscopy. NMR differs from other spectroscopy because nuclear spin states are only present in the presence of magnetic field**.** All nuclei carry a charge. In some nuclei this charge spins on the nuclear axis, and this circulation of nuclear charge generates a magnetic dipole along the axis. Nuclei with a spin number, I of ½ (such as $^{1}\mathrm{H}$ and $^{13}\mathrm{C}$) possess a uniform spherical distribution while spin number I with 1 or more, have a non-spherical charge distribution. In quantum mechanical terms, the spin number determines the number of orientations that a nucleus may assume in an external uniform magnetic field, B in accordance with the formula $2\mathrm{I}+1$. A proton with spin number, $\mathrm{I}=\frac{1}{2}$, will have two energy levels (α and β spin states) as shown in figure 2

[18]. α and β spin states are degenerate, only in the static magnetic field, but this degeneracy is destroyed as a result of the interaction of the nuclear moment, μ with B. In an applied magnetic field, all protons have their magnetic moments either aligned with the field as in $\alpha = +\frac{1}{2}$ or opposed to it (the higher energy anti-parallel orientation) as in $\beta = -\frac{1}{2}$.

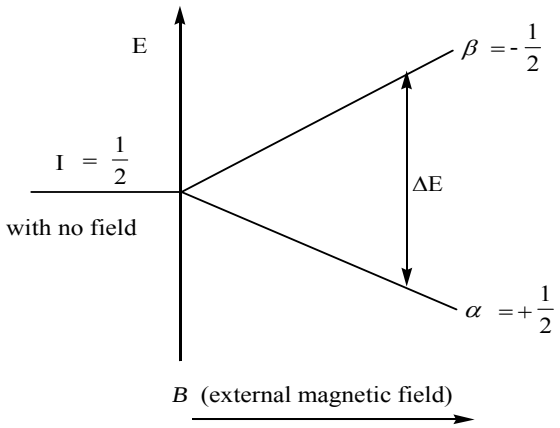

Figure 2. Energy separation between nuclear states for a proton in a magnetic field

The fundamental NMR equation correlating electromagnetic field strength, B and the frequency of electromagnetic radiation, v is given by the Larmor equation 1.18

$$v = \frac{\gamma B}{2\pi} \qquad (1.18)$$

where γ is the magnetogyric ratio which is a characteristic of a particular nucleus and it is a proportionality constant between the magnetic moment, μ and the spin number I as $\gamma = \frac{2\pi\mu}{h\mathrm{I}}$. Resonance frequency (the key feature of NMR) is directly proportional to the strength of the applied magnetic field. The most important perturbation of the NMR frequency for applications of NMR is the shielding effect of the surrounding electrons that reduces the magnetic field at the nucleus and thereby the frequency and energy gap required to achieve resonance is also reduced. This shift in the NMR frequency due to the electrons molecular orbital coupling to the external magnetic field is called chemical shift. The difference between the applied magnetic field and the field at the nucleus is termed the nuclear shielding.

The quantities of primary interest in due course are the nuclear magnetic shielding tensor which is defined as the mixed second derivatives of energy, E, with respect to the magnetic moment of ith nucleus, $\overrightarrow{m_i}$ and the external magnetic field, $\vec{B}$:

$$\sigma_i^{\alpha\beta} = \frac{\partial^2 E}{\partial B^{\alpha} \partial m_i^{\beta}} \tag{1.19}$$

where α and β are the corresponding vector or tensor components of the external magnetic field and induced magnetic moment respectively [19].

The derivative formulation is the easiest method for calculating the effect of a perturbation. In this case the energy is expanded in a Taylor series in the perturbation strength λ, [3]

$$E(\lambda) = E(0) + \frac{\partial E}{\partial \lambda}\lambda + \frac{1}{2}\frac{\partial^2 E}{\partial \lambda^2}\lambda^2 + \frac{1}{6}\frac{\partial^3 E}{\partial \lambda^3}\lambda^3 + \ldots \tag{1.20}$$

The perturbation is usually a vector, the second derivative a matrix and the third derivative a tensor, and so on. A tensor is useful for describing the relation ship between two vectors such as the spin interactions in NMR. The magnetic field at the nucleus (B_{nuc}) and the external magnetic field (B_{ext}) are related by NMR shielding tensor σ (a 3x3 matrix) as follows

$$\vec{B}_{nuc} = \sigma \vec{B}_{ext} \tag{1.21}$$

$$\begin{bmatrix} B_x \\ B_y \\ B_z \end{bmatrix}_{nuc} = \begin{bmatrix} \sigma_{xx} & \sigma_{xy} & \sigma_{xz} \\ \sigma_{yx} & \sigma_{yy} & \sigma_{yz} \\ \sigma_{zx} & \sigma_{zy} & \sigma_{zz} \end{bmatrix} \begin{bmatrix} B_x \\ B_y \\ B_z \end{bmatrix}_{ext} \tag{1.22}$$

Upon choosing the principal axis system in which the tensor is diagonal, the trace of a tensor, $\mathrm{Tr}\,\sigma$ is given as [19]

$$\mathrm{Tr}\ \sigma = \sigma_{xx} + \sigma_{yy} + \sigma_{zz} \tag{1.23}$$

In conventional NMR experiments, it is very difficult to determine all the components of the chemical shielding, thus only the symmetric part of the shielding is determined. This is true in case of solution (liquid state NMR) because the molecules are rapidly tumbling. Hence, the isotropic (orientation-independent) chemical shielding, σ_{iso}, is given by the trace of a tensor [19,20] as

$$\sigma_{iso} = Tr\sigma = \frac{1}{3}\left(\sigma_{xx} + \sigma_{yy} + \sigma_{zz}\right) \tag{1.24}$$

where σ_{xx}, σ_{yy} and σ_{zz} are the eigenvalues of the shielding tensor. In theoretical calculations the isotropic chemical shielding, σ_{iso}, must then be subtracted from the shielding, σ_{ref} in the reference system, TMS in this case, both obtained at the same level of theory. Therefore, the nuclear magnetic shielding difference (the chemical shift), δ_i, is calculated [21,22] using the equation

$$\delta_i\left(ppm\right) = \frac{\nu - \nu_{ref}}{\nu_{ref}} = \frac{\gamma B}{2\pi}\left(\frac{\sigma_{ref} - \sigma_{iso}}{\nu_{ref}}\right) = a\left(\sigma_{ref} - \sigma_{iso}\right) \tag{1.25}$$

where ν and ν_{ref} represent the Larmor frequency for the compound of interest and reference respectively. a is a slope with magnitude of unity. Small molecules in solution can also show rapid tumbling that averages anisotropic interactions. Thus, the anisotropic (orientation-dependent) chemical shielding, σ_{anis}, is expressed by [20,22]

$$\sigma_{anis} = \sigma_{33} - \frac{1}{2}\left(\sigma_{11} + \sigma_{22}\right) \tag{1.26}$$

where $\sigma_{11} < \sigma_{22} < \sigma_{33}$ are eigenvalues of the shielding tensor.

A common difficulty in the calculation of magnetic properties implies the usual wave functions do not guarantee gauge invariance or simply, the results may depend on the position of the molecule in the Cartesian frame. The **GIAO** (gauge- Including/Independent or Invariant Atomic Orbitals) method [23, 24] is used for removing dependence on the coordinate system when computing NMR chemical shifts. This approach allows the computation of the absolute chemical shielding due to the electronic environment of individual nuclei. The results are not dependent on choosing an origin for the magnetic field.

Using the notation where the first and higher derivatives are denoted by superscripts specifying the variables of differentiation of equation (1.19), the general expression for the shielding tensor with nucleus N becomes [25]

$$\sigma_N^{ab} = Tr\left\{\mathrm{P}^{oo} \times h_N^{ab}\right\} + Tr\left\{\mathrm{P}^{ao} \times h_N^{ob}\right\} \tag{1.27}$$

where P is the reduced density matrix and h is the matrix of the one-electron part of the Hamiltonian and $ab\left(a,b = x,y,z\right)$ is the tensor components. The first term in equation (1.27) is the diamagnetic component of the shielding and the second term represents the paramagnetic part of the shielding which depends on the first order density matrix. The GIAO methodology, for calculating of magnetic properties in SCF, uses explicitly field-dependent basis functions of the form [25]:

$$\chi_\mu\left(\vec{B}\right) = \exp\left[-\frac{i}{2c}\left(\vec{B} \times \vec{R}_\mu\right) \cdot \vec{r}\right] \chi_\mu\left(\vec{o}\right) \tag{1.28}$$

where $\vec{R}_\mu$ is the position vector of basis function χ_μ and $\chi_\mu\left(\vec{0}\right)$ denotes the usual field-independent basis functions and c is the velocity of light. The derivative of a field-dependent basis functions with respect to the magnetic field direction i is

$$\chi_\mu^{B_i} = -\frac{i}{2c}\left(\vec{R}_\mu \times \vec{r}\right)_i \chi_\mu\left(\vec{o}\right) \tag{1.29}$$

1.4.2 Infrared (IR) Vibrational Spectroscopy

The portion of the infrared region most useful for analysis of organic compounds is the middle IR region which lies between 2.5μm (4000cm^{-1}) and 50μm (670cm^{-1}). Most of the time the vibrational IR region of the electromagnetic spectrum is expressed interms of wavenumber, $\tilde{\nu}$, with units of cm^{-1}. The vibrational frequency (wave number), $\tilde{\nu}_{vib}$, obtained from quantum mechanical solution of a harmonic oscillator energy eigenvalues is given by

$$\tilde{\nu}_{vib} = \frac{1}{2\pi c}\sqrt{\frac{k}{\mu}} \tag{1.30}$$

where the reduced mass, $\mu = \frac{m_1 m_2}{m_1 + m_2}$ in grams and force constant, k in dynes/cm. Therefore, the exact frequency at which a given vibration occurs is determined by the strengths of the bonds involved (force constant) and the mass of the component atoms

(reduced mass). Generally, the following points are important in IR vibrational frequency [26].

1. Stronger bonds have a larger force constant, and thereby vibrate at higher frequencies than the weaker bonds
2. Bonds between atoms of higher masses (larger reduced mass) vibrate at lower frequencies than bonds between lighter atoms.
3. Bending vibrations occur at lower energy than stretching vibrations due to the lower value for the bending force constant and asymmetric stretching vibrations occur at higher frequencies than symmetric stretching vibrations.
4. Resonance has the effect of reducing the force constant and hence lowers the frequency.
5. Hybridization affects the frequency such that $sp > sp^2 > sp^3$ interms of bond strength.

As selection rule, a vibrational transition is said to be IR active, if the dipole moment of the molecule changes during vibration. Absorption bands associated with C=O bond stretching are usually very strong because a large change in the dipole takes place in that mode. IR spectroscopy is a powerful tool for identifying aromatic compounds. The existence of one or more aromatic rings in a structure is normally determined from the C-H and C=C-C ring-related vibrations. A molecule composed of N-atoms has 3N degrees of freedom, six of which are translations and rotations of the molecule itself. Non-linear polyatomic molecule has 3N-6 fundamental modes of vibrations. However, the number of normal modes of vibration is less than this value since several vibrations are redundant or regenerate. The complexity of infrared spectra in the fingerprint (1300 to 900cm^{-1}) region is normally due to this situation. The successful interpretation of IR spectra is based on both the presence and absence of important bands [27]. The functional group region is generally found at higher-frequency region between 4000cm^{-1}-1300cm^{-1}.

1.4.3 Ultraviolet (UV) absorption spectroscopy

Most organic molecules and functional groups are transparent in the portions of the electromagnetic spectrum called UV/Visible region which ranges from 200nm to 800nm [28]. Electromagnetic radiation in this region enables one to analyze electronic structure of compounds since the energy of electromagnetic radiation in this region is able to cause electronic promotion. The energy of photon absorbed is related to the extent of conjugation and other functional groups of the compound. Generally, energetically favored electron promotion will be from the highest occupied molecular orbital (HOMO) to the lowest unoccupied molecular orbital (LUMO), and the resulting species is called an excited state. Electronic excited states are most relevant when considering absorption spectroscopy. Molecules can absorb a photon in the UV-Vis range and convert to an electronically excited state. The commonly used law in UV absorption spectroscopy is the Beer-Lambert law which is given by [29]

$$A = -\log_{10} \mathrm{T} = \varepsilon c \ell \tag{1.31}$$

where the transmittance, T is the ratio of the intensity of the transmitted to the incident monochromatic radiation, c is concentration (M) and ℓ path length (cm) of the sample, ε is molar extinction coefficient ($\mathrm{Lmol^{-1}cm^{-1}}$). An alternative measure of absorption intensity, which can be related readily to theoretical principles is the Oscillator Strength (the measure of intensity), f , given by

$$f = 4.315 \times 10^{-9} \int \varepsilon dv \tag{1.32}$$

The oscillator strength is useful for comparing different transitions. Oscillator strength can range from 0 to 1, or a small integer. A strong transition will have an f value close to 1. Oscillator strengths greater than 1 result from the degeneracy of real electronic systems. The major difference between the oscillator strength (dimensionless), f and extinction coefficient, ε is that f is a measure of the integrated intensity of absorption over a whole band, whereas ε is a measure of the intensity of absorption for a single wave length. The probability of a given transition is proportional to the square of the transition moment, T.M, $\int \psi_i \hat{\mu} \psi_f d\tau$ with the dipole moment, $\hat{\mu} = e\sum r_j$ for electronic charge e and r_j distance

between the two electrons. Quantum mechanically this transition moment is related to the oscillator strength as [30]

$$f = \frac{8\pi^2 \nu_{if} m_e \langle \psi_i \left| \hat{\mu} \right| \psi_f \rangle^2}{3he^2} \tag{1.33}$$

with m_e electronic mass, h Plank's constant and ν_{if} is the frequency corresponding to the transition.. Transition moment, T.M, is an approximate of three separate integrals as given by the following equation

$$\text{T.M} = \int \theta_i \theta_f d\tau_N \int S_i S_f d\tau_s \int \varphi_i \hat{\mu} \varphi_f d\tau_e \tag{1.34}$$

The first and second terms in equation (1.34) represents overlap integral of the wavefunction for nuclear vibrations and spin overlap integral respectively, while the third integral refers to electronic transition moment which depends on symmetries and amount of overlap of the initial and final spatial orbitals. If one of the integrals of this equation is zero (a zero of probability occurrence), the transition is forbidden, otherwise allowed. For an electronic transition to take place two conditions must be satisfied. (a) A molecule must absorb a photon of radiation with energy that is equal to the difference between the HOMO and the LUMO of the ground state. The energy difference ΔE_{f_i} between electronic final state, ψ_f and initial state, ψ_i is, therefore, given by

$$\Delta \text{E}_{f_i} = \text{E}_{LUMO} - \text{E}_{HOMO} = \hbar\omega \tag{1.35}$$

where ω is frequency of electromagnetic radiation and (b). The franc-condon integral should be different from zero.

Common types of electronic transitions and their energy order for bonding orbitals (σ, π), non-bonding (n) orbitals and anti-bonding orbitals (π^*, σ^*) are shown in figure 1 [29,30].

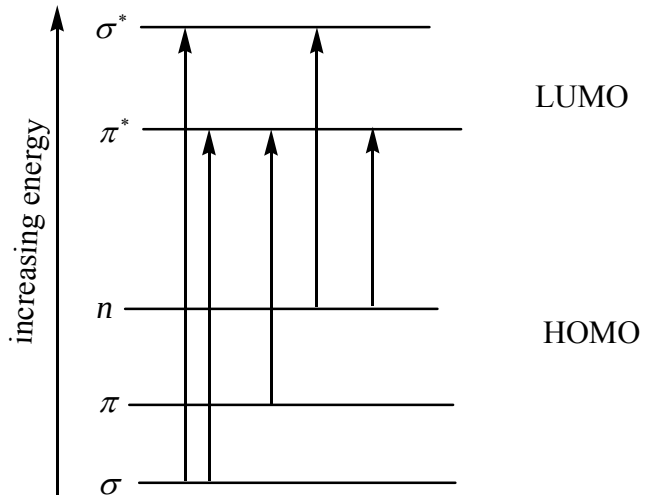

Figure 3. Common types of electronic transitions

2. Objectives of the project

This project was performed mainly for the purpose of the following general and specific objectives.

2.1 General objective

To compute the molecular properties of naturally occurring homoisoflavonoids

2.2 Specific objectives

A. To find the structure of the six-membered heterocyclic ring that is common in all naturally occurring homoisoflavonoids.

B. To determine ^{1}H and ^{13}C chemical shifts of five homoisoflavonoids

C. To calculate the infrared absorption frequencies of five homoisoflavonoids

D. To compute the ultraviolet (UV) electronic transition so as to define the types of electronic transitions involved in these compounds of interest.

3. Computational methods

All calculations were done by using Gaussian03W [31]. The compounds of interest were first optimized before any type of chemical properties has been determined. The ^{1}H and ^{13}C NMR shielding tensors (chemical shifts) were determined using GIAO method at HF and DFT levels using the 6-311+G (2d, p) basis set. Chemical shifts were calculated with respect to the reference, TMS, compound. The IR absorption frequencies of homoisoflavonoids were obtained using DFT/B3LYP/6-31G (d) and the results were multiplied by a scaling factor of 0.9614. In the UV electronic transitions, calculations of excited states were performed using the Time-Dependent Density Functional Theory (TD-DFT) with B3LYP/6-31G(d) formalism as implemented in the Gaussian03 code.

This project was done using the dual core Intel[R] Pentium[R] 4 CPU Version 2002 computer.

4. Results and discussion

4.1. Geometry optimization results

The optimized molecular structures and atom labeling of homoisoflavonoids are given in figure 4.

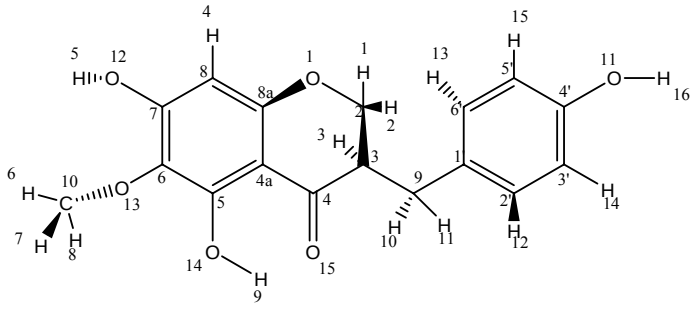

5, 7-dihydroxy-6-methoxy-3-(4'-hydroxybenzyl) chroman-4-one (**A**)

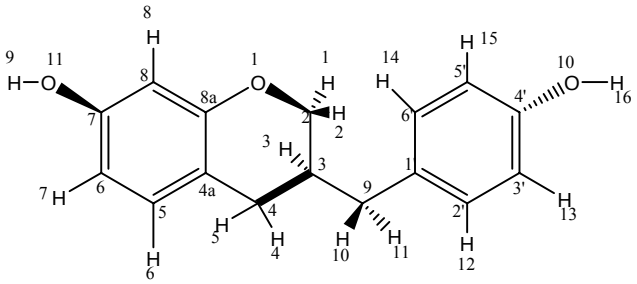

7-hydroxy-3-(4'-hydroxybenzyl) flavone (**B**)

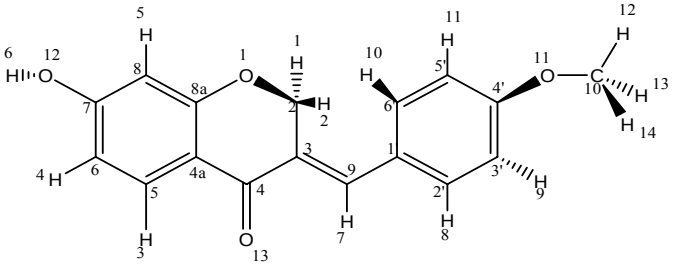

(E)-7-hydroxy-3-(4'-methoxybenzylidene) chroman-4-one (**C**)

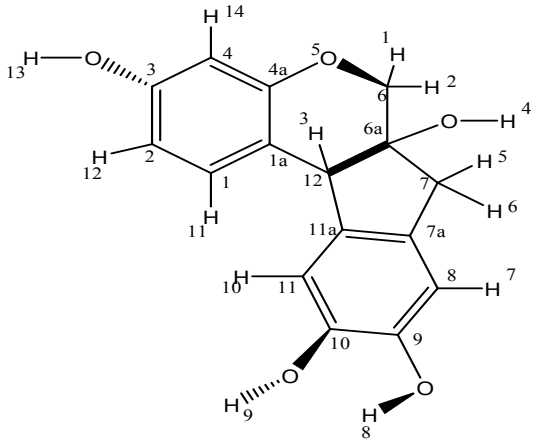

Brazilin (7, 11b-dihydrobenz[b]indeno [1, 2-d] pyran-3, 6a, 9, 10, (6H)-tetrol) (**D**)

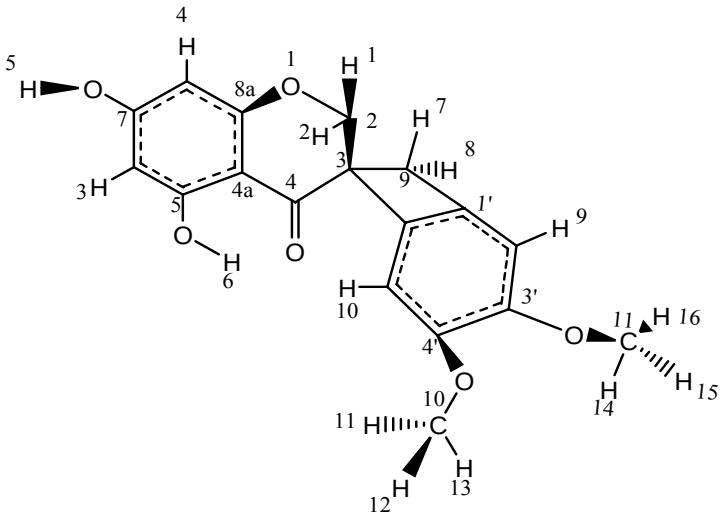

5, 7-hydroxy-3', 4'-dimethoxyspiro {2H-1-benzopyran-3-bicyclo [4.2.0] octa [1'.3'.5']-trien}-4-one (**E**)

Fig 4. Optimized molecular structures and atom labeling of the homoisoflavonoids

Geometry optimizations of these natural homoisoflavonoids have resulted in half-chair conformation of the six-membered heterocyclic ring of the chromanone moiety with equatorial phenyl ring at position carbon number 3; which is shown in figure 5.

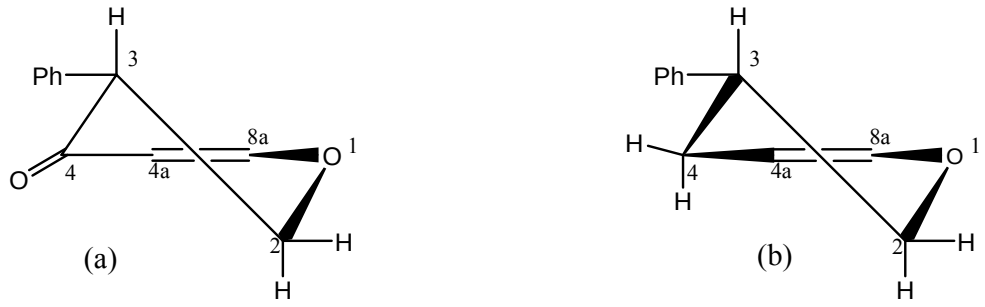

Figure.5. The generalized half-chair conformations adopted by the chromanone moiety for homoisoflavonoids (a) with carbonyl or (b) without carbonyl.

The aromatic part of the chromanone (pyrone) moiety is an invariant feature as compared to the six-membered heterocyclic ring. The x-ray crystallography results have also confirmed the half-chair or distorted sofa conformations of homoisoflavonoid structures [32, 33]. ^{1}H chemical shifts are sensitive probes for steric effects, reflecting differences in bond lengths, bond angles and dihedral angles in a systematic way [34]. Some selected optimized structural parameters of these compounds are given in table I below.

Table I. Selected optimized structural parameters (B3LYP/6-31G (d) level of theory) of homoisoflavonoids (Bond length (Å), bond angle and dihedral angle in (deg))

Parameters[a]	Homoisoflavonoids				
	A	**B**	**C**[b]	**D**	**E**
C2-C3 (6-6a)	1.5269	1.5270	1.51388(1.5037)	1.5205	1.5407
C3-C9 (6a-7)	1.5442	1.5437	1.3587(1.3412)	1.5405	1.5893
C9-C1' (7-7a)	1.5147	1.5131	1.4906(1.4671)	1.5275	1.4672
C3-C4 (6a-12)	1.5273	1.5375	1.5001(1.4846)	1.4953	1.5217
C1'-C2' (7a-8)	1.4011	1.4067	1.4281(1.3978)	1.3897	1.4424
C1'-C6' (7a-11a)	1.4023	1.4011	1.4198(1.3932)	1.3956	1.4431
C4-C4a (12-1a)	1.4476	1.5126	1.4836(1.4818)	1.5167	1.4621
C2-C3-C9 (6-6a-7)	112.78	111.63	126.09(126.65)	119.03	119.28
C3-C9-C1' (6a-7-7a)	113.77	114.44	130.41(128.33)	98.46	109.93
C4-C3-C9 (12-6a-7)	112.19	111.46	117.84(118.66)	101.18	119.96
C9-C1'-C6' (7-7a-11a)	121.58	121.36	123.01(122.70)	121.98	119.8
C9-C1'-C2' (7-7a-8)	120.79	120.78	118.91(119.07)	124.01	120.4
C2-C3-C9-C1' (6-6a-7-7a)	67.4	64.1	5.7(3.3)	-166.0	83.8
C2-C3-C4-C4a (6-6a-12-1a)	-29.0	-46.7	20.11(16.71)	-60.7	16.3
C9-C3-C4-C4a (7-6a-12-1a)	-154.7	-170.1	-154.08(-161.35)	173.4	174.8

[a] the parameters in brackets are for **D**. [b] values in brackets are experimental values for **C.**

From table I above the calculated parameters satisfy the distorted sofa or half-chair conformation of the chromanone (pyrone) ring with atom C-2 most off the plane of the ring. There is some what a significance difference in bond lengths, bond angles and dihedral angles among the homoisoflavonoids which reflects the influence of the substituents on the two phenyl rings. For compound **C** the two phenyl rings are linked by a non-planar *cisoid* 1, 3-enone bridge with calculated inclination angle of 62.3^{o} between the two phenyl rings which is in good agreement with the x-ray results. This is due to the intramolecular interactions between the hydrogens attached to C-2 and C-6'.

4.2 Molecular properties

4.2.1 ^{1}H and ^{13}C isotropic chemical shifts

An approximate value for the isotropic chemical shift of hydrogen (proton) for TMS is 32.42 and 31.88 ppm at HF/6-311+G (2d, p) and DFT/B3LYP/ 6-311+G (2d, p) levels of theory respectively. Moreover, the isotropic chemical shift for carbon of TMS is 194.61 ppm at HF and 182.46 ppm at DFT/B3LYP levels of theory. The calculation of chemical shift is carried out using CD_3COCD_3 solvent for compounds **A**, **B**, **C** and **D** as well as CD_3OD solvent for compound **E**.

Comparison of experimental and computed results of 5, 7-dihydroxy-6-methoxy-3-(4'-hydroxybenzyl) chroman-4-one (**A**) for ^{1}H and ^{13}C chemical shifts is given in table II. From table II (the first four columns) one can observe that the calculated ^{1}H chemical shift values of 12 data points for HF and DFT/B3LYP levels of theory using the same basis set 6-311+G (2d, p) with GIAO method have a mean error of 0.25 and 0.22 ppm respectively. Hence the DFT/ B3LYP method shows the best fit with the experiment. The largest differences between experimental and calculated ^{1}H shifts for HF and DFT/B3LYP methods are for protons of numbers 9 and 11 with differences of 0.46 and 0.52 ppm respectively. Since these protons are influenced by interactions from the aromatic rings and carbonyl of the chromanone ring. The chemical shift of hydrogens in one methoxy group are scattered in simulation, but they show the same order as the experimental when those chemical shifts are averaged. As in ^{1}H the largest differences between experimental and calculated ^{13}C for HF and DFT/B3LYP methods are for carbons of numbers 6 and 8a with differences of 10.2 and 8.2 ppm respectively.

TableII.[1]H and [13]C chemical shifts for 5, 7-dihydroxy-6-methoxy-3-(4'-hydroxybenzyl) chroman-4-one (**A**)

Atom (H)	Computed results (ppm)		Expt'l (ppm)[a]	atom (C)	Computed results (ppm)		Expt'l (ppm)[a]
	GIAO/HF[m]	GIAO/ B3LYP[m]			GIAO/HF[m]	GIAO/ B3LYP[m]	
1	4.09(0.2)	4.18(0.11)	4.29	2	62.1(8.0)	74.6(-4.5)	70.1
2	3.69(0.5)	3.94(0.25)	4.19	3	43.4(4.0)	52.9(-5.5)	47.4
3	2.77(0.14)	2.81(0.1)	2.91	4	202.0(-2.2)	203.9(-4.1)	199.8
4	6.03(-0.08)	6.09(-0.14)	5.95	4a	96.4(6.5)	106.6(-3.7)	102.9
5	6.43	6.55	-	5	160.1(-3.4)	163.6(-6.9)	156.7
6,7,8	3.80(-0.04)	3.77(-0.01)	3.76	6	119.5(10.2)	133.0(-3.3)	129.7
9	11.90(0.46)	12.75(-0.39)	12.36	7	163.2(-3.3)	166.3(-6.4)	159.9
10	2.99(0.14)	2.63(0.5)	3.13	8	89.8(5.5)	96.2(-0.9)	95.3
11	3.09(-0.42)	3.19(-0.52)	2.67	8a	162.7(-3.2)	167.7(-8.2)	159.5
12	7.38(-0.28)	7.32(-0.22)	7.10	9	27.6(4.7)	34.5(-2.2)	32.3
13	7.29(-0.19)	7.25(-0.15)	7.10	10	54.4(6.4)	60.4(0.4)	60.8
14	6.60(0.2)	6.77(0.03)	6.80	1'	126.9(3.1)	137.7(-7.7)	130.0
15	7.13(-0.33)	7.05(-0.25)	6.80	2',6'	131.5(-0.5)	134.1(-3.1)	131.0
16	3.74	3.89	-	3',5'	113.2(3.0)	117.9(-1.7)	116.2
-	-	-	-	4'	153.2(3.9)	158.6(-1.5)	157.1
Mean error	0.25	0.22			4.52	4.00	

[a] reference [35] and [m]6-311+G (2d, p)

More electronegative oxygen atom (O-15) of the C=O group results in the formation of strong hydrogen bonding while the other more electronegative oxygen atom of the hydroxyl group leads to weaker acidic group, which results in weaker hydrogen bonding. Hence, hydrogen bonding is formed between O-H (H-9) which is closer the carbonyl group and carbonyl oxygen (O-15) and thereby responsible for the downfield of H-9 having a calculated proton chemical shift value of 12.75 ppm using GIAO/B3LYP/6-311+G (2d, p) method or 12.36 ppm determined experimentally as shown in table II. Generally, electron

withdrawing groups decrease intramolecular hydrogen bond strength while π systems like the phenyl group increase the hydrogen bond strength [36].

Comparison of experimental and computed (GIAO/HF and GIAO/B3LYP) for DFT/B3LYP optimized geometry) results of 7-hydroxy-3-(4'-hydroxy- benzyl) flavone (**B**) for ^{1}H and ^{13}C chemical shifts is given in table III.

Table III. ^{1}H and ^{13}C chemical shifts for 7-hydroxy-3-(4'-hydroxybenzyl) flavone (**B**)

Atom (H)	Computed results (ppm)		Expt'l (ppm)[b]	atom (C)	Computed results (ppm)		Expt'l (ppm)[b]
	GIAO/HF[m]	GIAO/ B3LYP[m]			GIAO/HF[m]	GIAO/ B3LYP[m]	
1	4.30	4.23	4.04	2	74.16	68.9	70.72
2	3.91	3.69	3.66	3	39.3	33.2	35.48
3	2.40	2.18	2.09	4	37.7	31.1	31.11
4	2.95	2.65	2.60	4a	120.3	115.4	113.96
5	2.36	2.34	2.23	5	133.4	136.1	131.35
6	6.98	6.78	6.75	6	113.3	109.7	108.94
7	6.44	6.32	6.29	7	161.3	155.7	156.93
8	6.22	6.22	6.20	8	108.7	104.9	103.59
9	3.91	3.87	-	8a	160.8	158.3	156.18
10	3.14	2.83	2.51	9	38.8	40.1	37.82
11	2.61	2.50	2.45	1'	136.2	129.8	131.63
12,14	7.32	7.13	6.96	2',6'	131.0	133.1	130.86
13,15	7.11	6.92	6.72	3',5'	116.1	120.0	115.98
16	3.86	3.75	-	4'	162.0	154.4	156.13
Mean error	0.26	0.11			4.79	2.35	

[b] reference [37] [m] 6-311+G (2d, p)

Unlike the other class of homoisoflavonoids, flavans do not have a carbonyl group on the six-membered heterocyclic ring and due to this difference the spectral properties of 7-

hydroxy-3-(4'-hydroxybenzyl) flavone (**B**) is quite different from that of the 5,7-dihydroxy-6-methoxy-3-(4'-hydroxybenzyl)chroman-4-one (**A**). The ^{13}C NMR spectra of these two compounds (tables II &III) showed that the computed chemical shift for C-4 using the hybrid DFT method is at around 35.5 ppm and 203.9 ppm respectively for the former and later compounds. The computed chemical shifts in Table III especially, those results done using DFT/B3LYP, gives good fit with the experimental chemical shifts for both ^{1}H and ^{13}C NMR spectra. The calculated ^{1}H chemical shift values for 12 data points has found to be with a mean error of 0.26 and 0.11 ppm for HF/6-311+G (2d, p) and B3LYP/6-311+G (2d, p) methods respectively. The same ^{1}H chemical shift values for the pairs of proton numbers 13&15 and 12&14 as well as the carbon numbers corresponding to these protons form an AA'BB' system. Moreover, the mean error for the computed ^{13}C NMR spectra is found to be 4.79 and 2.35 ppm as the above respective order.

The experimental and computed chemical shift results (^{1}H and ^{13}C chemical shifts) for (E)-7-hydroxy-3-(4'-methoxybenzylidene) chroman-4-one (**C**) using HF and DFT/B3LYP/6-311+G (2d, p) methods are given in table IV. The NMR spectrum (^{1}H and ^{13}C with respect to TMS) of (E)-7-hydroxy-3-(4'-methoxybenzylidene) chroman-4-one(**C**), commonly known as bonducellin, is best computed with hybrid DFT methods and gives a best fit with the experimental results. The protons present in methoxy group have an average chemical shift around 3.78 ppm and only with a deviation of 0.10 ppm from experiment when computed at DFT level of theory. The calculated chemical shift for H-1 of compound **C** is about 5.45 ppm as compared to 5,7-dihydroxy-6-methoxy-3-(4'-hydroxybenzyl)chroman-4-one which is 4.18 ppm for the same proton. This may be due to the presence of pi-electron system on the former than the later. In addition the O-H proton (H-6) attached to C-7 has a chemical shift value of 10.12 ppm indicating that this proton is involved in hydrogen bonding (may be with the solvent) or the lone pair of oxygen, O-12 is delocalized with the ring system. The ^{13}C spectra given in table IV indicate the computed results have a mean error of 4.10 and 2.82 ppm at HF and DFT/B3LYP levels of theory respectively, while for proton NMR, the mean errors are found to be 0.66 and 0.31 ppm for the HF and DFT methods.

Table IV. ^{1}H and ^{13}C chemical shifts for (E)-7-hydroxy-3-(4'-methoxybenzylidene) chroman-4-one (**C**)

Atom (H)	Computed results (ppm)		Expt'l (ppm)[c]	atom (C)	Computed results (ppm)		Expt'l (ppm)[c]
	GIAO/HF[m]	GIAO/ B3LYP[m]			GIAO/HF[m]	GIAO/ B3LYP[m]	
1	4.78	5.45	5.35	2	64.1	65.1	67.2
2	4.4	5.21	-	3	122.2	123.6	126.6
3	8.61	8.31	7.85	4	182.5	182.2	180.2
4	6.39	6.70	6.62	4a	109.2	111.0	114.2
5	5.65	6.05	6.40	5	132.1	127.3	129.2
6	8.55	9.07	10.12	6	106.7	106.3	110.8
7	8.12	8.31	7.69	7	168.8	159.9	164.3
8, 10	7.19	7.34	7.42	8	99.0	98.7	102.4
9, 11	6.92	7.05	7.07	8a	168.2	159.37	162.5
12,13 & 14	3.40	3.78	3.88	9	139.9	129.9	136.5
-	-	-	-	10	48.8	51.9	54.9
-	-	-	-	1'	121.2	127.2	128.5
-	-	-	-	2',6'	136.2	133.0	131.4
-	-	-	-	3',5'	114.3	113.2	113.7
-	-	-	-	4'	155.9	157.8	159.9
Mean error	0.66	0.31			4.10	2.82	

[c] reference [38] and [m] 6-311+G (2d, p)

The NMR spectral data (^{1}H and ^{13}C chemical shifts) of brazilin computed at HF and DFT/B3LYP levels of theory using GIAO method is given in table V.

Table V. ^{1}H and ^{13}C chemical shifts of Brazilin (**D**)

Atom (H)	Computed results (ppm)		Expt'l (ppm)[d]	atom (C)	Computed results (ppm)		Expt'l (ppm)[d]
	GIAO/HF[m]	GIAO/ B3LYP[m]			GIAO/HF[m]	GIAO/ B3LYP[m]	
1	4.17	4.11	4.10	1	129.8	133.1	132.3
2	3.62	3.78	3.87	1a	118.1	119.0	115.8
3	4.22	4.10	4.14	2	110.5	112.7	110.0
4	3.51	3.89	-	3	158.2	157.2	155.8
5	3.08	2.96	2.97	4	101.7	103.8	104.3
6	3.20	3.21	3.18	4a	158.7	157.3	157.9
7	7.03	6.92	6.81	6	76.1	72.6	71.0
8	3.01	3.55	-	6a	81.0	77.7	78.1
9	2.99	3.41	-	7	43.2	44.0	43.1
10	6.89	6.78	6.92	7a	132.5	131.4	131.7
11	7.52	7.32	7.35	8	117.3	115.7	113.0
12	6.77	6.72	6.66	9	146.2	144.9	145.4
13	2.87	3.08	-	10	145.8	145.8	145.1
14	6.50	6.39	6.46	11	110.1	111.8	112.6
-	-	-	-	11a	143.2	138.1	137.6
-	-	-	-	12	48.7	54.2	51.3
Mean error	0.11	0.06			2.26	1.22	

[d] reference [39] and [m]6-311+G (2d, p)

Both the calculated ^{1}H and ^{13}C NMR chemical shifts of Brazilin at HF and DFT/B3LYP levels of theories are in very good agreement with the experimentally determined values when using the DFT/B3LYP method and have mean errors of 1.22 and 0.06 ppm for ^{13}C and ^{1}H chemical shifts respectively.

From the ^{1}H NMR data of brazilin the six membered heterocyclic ring is found to be half-chair and thereby confirming most stable structure, requiring the 6α-H to be axial upwards since it believes steric repulsion between the hydrogens H-3 and hydrogens of C-6 (H-1 and H-2) which is evident in the half-boat conformation of the six membered heterocyclic ring. The resonance for H-3 calculated at DFT/B3LYP level of theory is 4.10 ppm and almost overlaps with the H-1 proton on C-6. Hence, the nature of the ring fusion of six membered heterocyclic ring and the five membered ring are stabilized as cis orientation. The entire above phenomenon are in agreement with the experimental explanation.

The NMR spectral data for compound **E** is given in table VI which is computed at the same level of theory as the above four homoisoflavonoids and compares computed results with the experimentally determined values and are fairly comparable. The proton NMR spectra of compound **E** showed two sets of doublets resonating at calculated value of 4.52 and 5.55 ppm for H-1 and H-2 as well as the H-7 and H-8 with 3.70 and 2.70 ppm respectively. The computed values for the broad singlet protons H-3 and H-4 are obtained with 6.71 and 6.46 ppm at DFT/B3LYP/6-311+G (2d, p) level of theory and thereby show good agreement with the experiment. Moreover, table VI showed that the calculated ^{1}H chemical shift values of 9 data points at HF and DFT methods with mean errors of 0.62 and 0.46 ppm respectively. The chemical shift of hydrogens in each of the two methoxy groups are scattered in simulation, but they show the same order as the experimental when those chemical shifts are averaged.

Table VI. ^{1}H and ^{13}C chemical shifts for 5, 7-dihydroxy-3', 4'-dimethoxyspiro {2H-1-benzopyran-3-bicyclo [4.2.0] octa [1.3.9]-trien}-4-one (**E**)

Atom (H)	Computed results (ppm)		Expt'l (ppm)[e]	atom (C)	Computed results (ppm)		Expt'l (ppm)[e]
	GIAO/HF[m]	GIAO/ B3LYP[m]			GIAO/HF[m]	GIAO/ B3LYP[m]	
1	5.3(-0.74)	4.52(0.04)	4.56	2	72.26(1.44)	69.43(4.27)	73.7
2	4.72(-0.22)	5.55(1.05)	4.50	3	61.61(7.2)	51.33(3.07)	54.4
3	6.01(-0.22)	6.71(-0.92)	5.79	4	204.2(-8.12)	192.7(3.4)	196.1
4	5.66(0.42)	6.46(-0.65)	5.81	4a	99.32(1.38)	104.31(3.61)	100.7
5	2.79	3.92	-	5	161.98(0.82)	160.20(2.6)	162.8
6	6.26	7.44	-	6	96.47(1.17)	100.61(5.31)	95.3
7	4.83(-1.29)	3.70(-0.16)	3.54	7	161.20(3.7)	166.3(-1.4)	164.9
8	4.79(-1.75)	2.70(0.34)	3.04	8	90.28(2.22)	94.6(-2.1)	92.5
9	6.91(-0.02)	7.25(-0.36)	6.89	8a	161.64(2.26)	160.6(3.3)	163.9
10	6.57	7.30	-	9	44.4(9.1)	30.7(4.6)	35.3
11,12, &13	4.26(-0.53)	3.49(0.24)	3.73	10, 11	54.66(1.23)	52.3(3.6)	55.9
14,15 &16	3.35(0.46)	3.39(0.42)	3.81	1'	135.32(-0.72)	133.4(1.17)	134.6
-	-	-	-	2'	116.37(-7.87)	107.86(0.64)	108.5
-	-	-	-	3'	145.05(6.45)	151.69(-0.19)	151.5
-	-	-	-	4'	147.59(2.71)	152.01(-1.71)	150.3
-	-	-	-	5'	109.4(-2.7)	105.97(0.73)	106.7
-	-	-	-	6'	142.29(-5.99)	138.20(-1.9)	136.3
Mean error	0.62	0.46			3.81	2.56	

[e] reference [40] and [m]6-311+G (2d, p)

The calculated mean errors for ^{13}C chemical shifts of 17 data points using HF and DFT/B3LYP levels of theory in their respective order are found to be 3.81 and 2.56 ppm.

In both cases the hybrid DFT method dominates over the HF method in chemical accuracy.

4.2.2 IR vibrational frequency results

Since, the infrared absorption frequencies calculated computationally in this project work is done using the harmonic oscillator approximation, to fit this approximation with the experimental results a linear scaling factor 0.9614 (B3LYP/6-31G (d)) have been used. Typical gas-phase infrared absorption frequencies of five homoisoflavonoids, **A**, **B**, **C**, **D** and **E** are given in table VII. Only the main high intensity IR bands are tabulated though a number of low intensity bands are structural part of the given molecules of interest and these are briefly explained.

The computed infra-red spectrum of **A** shows three O-H stretching bands for which one strong band at 3607 cm^{-1}(free-O-H) and two broad bands at 3354 cm^{-1}, 3512 cm^{-1} for the hydrogen bonded H-9 and O-H group attached to C-7 (H-5) respectively. This is supported by the presence of small broad bands ranging from 1338-1412 cm^{-1} which represent the presence of in-plane O-H bending vibrations. The existence of non-aromatic CH stretching is suggested by the occurrence of the bands at 2912, 2879 and 1429 cm^{-1}, whereas the aromatic C-H absorption frequency bands occurs at around 3015 cm^{-1} and 968 cm^{-1}. Moreover, the C=C absorption frequency of the aromatic part have showed two absorption bands calculated to be at around 1608 cm^{-1} and 1511 $cm^{-}1$. The C=O stretching band at 1641 cm^{-1} and C-O stretching band at 1172 cm^{-1} are the other main characteristic features in the IR vibrational spectra of 5,7-dihydroxy-6-methoxy-3-(4'-hydroxybenzyl)chroman-4-one (**A**). Benzene derivatives exhibit a number of characteristic absorptions in their infrared spectrum which can be diagnostically useful in determining both the extent and pattern of substitution. However, when strongly electron donating or electron withdrawing groups or even conjugation, are present, the characteristic patterns lose much of their diagnostic value. This is the case for the lowering of vibrational frequency of carbonyl with calculated value of 1641 cm^{-1}. The

main IR absorption frequencies of compound **A** are compared to their corresponding experimental suggested values as given in table VII.

Table VII. IR spectral data (cm^{-1}) of homoisoflavonoids computed at B3LYP/6-31G (d) level of theory scaled with 0.9614.

Compound[n]	**A**	**B**	**C**	**D**	**E**
υC=O	1641 (1634)[a]	-	1638(1615)[c]	-	1635(1633)[e]
υO-H	3607,3512, 3354 (3347)[a]	3611(3592)[b], 3380 (3357)[b]	3582 **1337(1330)**[c]	3387(3350)[d]	3477(3464)[e]
υC-H	2912	2998(2975)[b] 2931(2914)[b] 2841(2854)[b] **1462(1474)**[b] **1463(1458)**[b]	2983(2970)[c] **1483(1476)**[c]	2945,2901, 2910, **1444, 1489**	2951, 2867 **1453**
υC=H Ar	3015 **968**	3031(3025)[b] **897**	3078 **846(840)**[c]	3021,3034, 3039,3055& 3067	3022(3020)[e] **937(929)**[e]
υC=C	-	-	1663(1655)[c]	-	-
υC=C Ar	1608 (1600)[a] &1511(1507)[a]	1612(1601)[b]& 1507(1511)[b]	1611(1602)[c]& 1513(1510)[c]	1627(1610)[d]& 1512(1500)[d]	1644
υC-O	1172(1160)[a]	1131(1124)[b] 1042(1033)[b]	1171(1177)[c] 1160(1155)[c] 1121(1102)[c]	1118 &1198	1222(1216)[e]

[n]values in brackets are experimental results and bold numbers indicate bending vibrations. [a] reference [35], [b] reference [37], [c] reference [38], [d] reference [40] and [e] reference [41]. Ar represents for aromatic and υ for vibrational frequency.

The infrared spectrum of 7-hydroxy-3-(4'-hydroxybenzyl) flavone (**B**) showed that there is no peak around 1660-1805 cm^{-1} confirming the absence of carbonyl group in its structure. Unfortunately, there are a number of non-aromatic C-H stretching bands at 2998, 2931,

2841 cm^{-1} and bending vibrations at 1462 and 1463cm^{-1} with additional C-O stretching vibration bands around 1131 and 1042 cm^{-1} as shown in table VII. However, the aromatic C-H part absorbs at higher frequency of about 3031 cm^{-1} and a medium intensity bending vibration at 897 cm^{-1} due to an out-of-plane wagging motion of all the C-H bonds. Its infrared absorption spectrum also contained two hydroxyl bands at 3611, and 3380 cm^{-1} and the usual aromatic C=C absorption band at around 1612 &1507 cm^{-1}. All of the computed results coincide in good agreement with the experimental results.

The IR spectrum of olefinic double bond of (E)-7-hydroxy-3-(4'-methoxybenzylidene) chroman-4-one (**C**), is characterized by the C=C stretching with a strong absorption at a calculated value of around 1663cm^{-1} and the out-of-plane C-H deformation (para substituted benzene ring) around 846 cm^{-1}which are in good agreement to the experimentally determined value. The strong absorption peaks at 1638 cm^{-1} of the carbonyl group, C=O stretch, is the other dominant characteristic phenomenon of the compound. Moreover, the infrared absorption spectrum contained the free hydroxyl band at 3582 cm^{-1} and its bending (in-plane) at around 1337 cm^{-1}, and the =C-H stretching at 3078 cm^{-1} or the C=C-C aromatic ring stretch at 1611 and 1513 cm^{-1} are obtained as a result of the DFT/B3LYP/6-31G(d) level of theory. The agreement of the above calculated vibrational intensities with the experimentally defined values is an indicative of actual structure of the compound via a good optimized geometry. The infrared absorption spectrum frequency of carbonyl group is lower than the usual diagnostic value of carbonyl of ketone. This is due to the influence of conjugation in that the double bond becomes partial double bond and thereby the force constant tends to decrease. As a consequence of this, the vibrational frequency decreases reasonably. Generally, only small changes in any preceding frequency absorptions are found in going from gases to condensed phases or in changing from one solvent to another [42].

Brazilin shows a strong IR absorption frequency band at 3387cm^{-1} for O-H stretch and two strong bands at around 1627 $cm^{-1}$and 1512 cm^{-1} for the aromatic C=C ring stretch and thereby indicates a smooth agreement with the experimental evidences as shown in table VII. There are also a number of weak phenyl ring substitution overtones at 1761, 1879,

1938, and 2001 cm^{-1} which is considered as fingerprint region. The position and shape of the O-H stretching bands are related to the potential energy function governing the motion of the proton. According to the computed results five bands in the 3070-3010 range which are assigned to the C-H stretching of the phenyl group.

The infrared absorption spectra of compound **E** showed that the strong band at 1635 cm^{-1} for the C=O stretching and a broad band at around 3477 cm^{-1} (O-H) are responsible for the formation of hydrogen bonding. The involvement of a carbonyl group in hydrogen bonding reduces the frequency of carbonyl stretching vibration by about 10 cm^{-1}. The difference between hydrogen bonded and free O-H frequencies is clearly related to the weakening of the O-H bond as a consequence of hydrogen bonding. The aromatic C-H stretching frequency band computed at B3LYP/6-31G (d) having a value of 3022 cm^{-1} and its bending vibrational frequency of about 937 cm^{-1}. 1644 cm^{-1} for C-H stretching of the aromatic ring and 1222 cm^{-1}that corresponds to C-O stretching frequency are the other main characteristic for the infrared absorption spectra of compound **E** which is tabulated in table VII.

4.2.3 UV electronic spectra results

The UV absorption spectra of homoisoflavonoids is characterized by the following chromophores: the three double bonded carbons of the aromatic part of the chromanone ring, the carbonyl at C-4, the carbons of the phenyl ring and nature of substituents attached at the two aromatic carbon rings. The rest low intensity absorption bands of homoisoflavonoids that is not tabulated in table VIII are quantum mechanically almost forbidden (very small f). Because of some overlap forbidden character, the $n \rightarrow \pi^*$ transitions have low probability and hence weak absorption bands (small f). The three more intense electronic excitation bands of each of the five naturally occurring homoisoflavonoids are given in table VIII.

Table VIII. Gas-phase excited states of homoisoflavonoids **A**, **B**, **C**, **D**, and **E (**using 6-31(d) optimized geometry) calculated with TD/B3LYP/ 6-31G (d) method.

Compound	States	λ (nm)	E (eV)	f
A	1	342.87 (328)[a]	3.6161	0.0374
	2	274.10 (290)[a]	4.5233	0.3181
	3	241.30 (222)[a]	5.1382	0.0302
B	1	247.29 (281)[b]	5.0137	0.0388
	2	241.66	5.1306	0.0292
	3	210.38 (225)[b]	5.8933	0.0381
C	1	364.16 (358)[c]	3.4047	0.0385
	2	337.97 (318)[c]	3.6685	0.3867
	3	308.27 (315)[c]	4.0219	0.2221
D	1	254.14 (292)[d]	4.8784	0.0116
	2	249.56	4.9681	0.0885
	3	213.73	5.8009	0.0915
E	1	270.40 (293)[e]	4.5853	0.1298
	2	266.17 (235)[e]	4.6580	0.2268
	3	242.91	5.1041	0.0778

[a] reference [43], [b] reference [37], [c] reference [38], [d] reference [40] and [e] reference [41] are experimental results (values in brackets)

As shown in table VIII, homoisoflavonoids **A**, **C** and **E** can have $n \rightarrow \pi^*$ transition of weak to medium intensity bands at wavelengths 342.87, 364.16 and 270 nm that correspond to 3.6161, 3.4047 and 4.5853 eV, respectively, and these confirming the presence of carbonyl compounds due to the excitation of an oxygen lone pair electron in to an unoccupied π-orbital. The additional auxochromes such as –OH and -OCH_3 attached at C-5 and C-6 leads to absorption maximum being shifted to longer wavelength (bathochromic shift) in compound **A** than compound **B**. The $\pi \rightarrow \pi^*$ and $n \rightarrow \pi^*$ are, generally, the UV electronic transition features of homoisoflavonoids.

Generally, the computed excited state wavelengths at TD-DFT/B3LYP/6-31G (d) method gives a good fit with the experimentally given values. Experimental evidence shows that hydroxyl group at C-5 as in **A** and **E**, have a significant effect giving bathochromic shift of about 40 nm due to hydrogen bonding between the phenolic hydrogen and the carbonyl oxygen at position C-4. If these hydroxyl groups are absent as in case **B,** the UV maxima tend to be shifted somewhat to shorter wavelength (hypsochromic shift). Computational results of this project also verify this truth.

5. Conclusion

A theoretical study of naturally occurring homoisoflavonoids has been performed quantum mechanically at the DFT/B3LYP level of theory though, in some cases, the HF method was also used for comparison. The optimized structural parameters of homoisoflavonoid **C** obtained by using B3LYP/6-31G (d) is in reasonable agreement with the x-ray data. Eventhough, the x-ray data or other theoretical results of the remaining compounds were not obtained; the agreement of computed molecular properties (NMR, IR & UV) with corresponding experimental results confirms the optimized structural parameters of these structures are correct. Overall, the calculated molecular properties show very good agreement with the experimental results. Since, the calculated molecular properties of naturally occurring homoisoflavonoids are in good agreement with the experimental values, it can, therefore, be conclude that the structures and molecular properties of these homoisoflavonoids have been reproduced through theoretical studies conveniently.

References

1. D. C. Young, *Computational Chemistry: A Practical Guide for Applying Techniques to Real-World Problems,* John Wiley & Sons, Inc., 2001.
2. W. Koch and M. C. Holthausen, *A Chemist's Guide to Density Functional Theory*, Wiley-VCH, 2000.
3. F. Jensen, *Introduction to Computational Chemistry*, John Wiley & Sons, Ltd., 1999.
4. M. R. Mueller, *Fundamentals of Quantum Chemistry: Molecular Spectroscopy and Modern Electronic Structure Computations*, Kluwer Academic Publishers, 2002.
5. W. B. Smith, *Introduction to Theoretical Organic Chemistry and Molecular Modelling,* Wiley-VCH, Inc., 1996.
6. F. D. Pacati and S. Boffi, *Phys. Rev.,* 1970, **C2**, 1205.
7. T. Clark, *A Handbook of Computational Chemistry*, John Wiley & Sons, Inc., 1985.
8. P. Caramella, K. N. Houk, and L. N. Domelsmith, *J. Am. Chem. Soc.*, 1977, **99**, 4511.
9. J. A. Pople, D. L. Beveridge, and P. A. Dobosh, *J. Chem. Phys.* 1967, **47**, 2026.
10. W. Kohn, *Rev. Mod. Phys.*, 1999, **71**, 1259.
11. R. G. Parr, and W. Yang, *Density Functional Theory of Atoms and Molecules*, Oxford University Press, Inc., 1989.
12. C. J. Cramer, *Essentials of Computational Chemistry*, John Wiley & Sons, Ltd., 2004.
13. J. B. Foresman and Æ. Frisch, *Exploring Chemistry with Electronic Structure Methods*, Gaussian Inc., 1996.
14. S. G. Sprag, J. Van-Staden, and K. Jager, *J. Ethnopharmacol.*, 2002, **80**, 95.
15. L. Farkas, A. Gottsegen, and M. Nogradi, *Tetrahedron*, 1970, **26**, 2787.
16. B. M. Abegaz, J. Mutanyatta-Comar and M. Nindi, *Natural Product Communications (NPC)*, 2007, **2**, 478.
17. S. J. Sup, K. J. Hee, L. Jiyong, and K. H. Jeong, *Planta Med*., 2004, **70**, 171.

18. H. Günther, *NMR Spectroscopy: Basic Principles, Concepts, and Applications in Chemistry*, John Wiley & Sons, Ltd., 1995.
19. D. Viki-Topic and L. Pejov, *Croatica Chemica Acta*, 2000, **73**, 1058.
20. E. E. Fileti, H. C. Georg, K. Coutinho and S. Canuto, *J. Braz. Chem. Soc.*, 2007, **18**, 75.
21. M. Sugimoto and H. Nakatsuji, *J. Chem. Phys*., 1995, **102**, 292.
22. R. H. Xie, G. W. Bryant, L. Jensen, J. Zhao, and V. H. Smith, *J. Chem. Phys*., 2003, **118**, 8632.
23. K. Wolinski, J. F. Hilton, and P. Pulay, *J. Am. Chem. Soc.*, 1990, **112**, 8252.
24. A. Hinchliffe, *Modelling Molecular Structures*, John Wiley & Sons, Ltd., 2000.
25. J. R. Cheeseman, G. W. Trucks, T. A. Keith, and M. J. Frisch, *J. Chem. Phys.*, 1996, **104**, 5497.
26. D. L. Pavia, G. M. Lampman and G. S. Kriz, *Introduction to Spectroscopy,* Thomson Learning, Inc., 2001.
27. J. Coates, *Interpretation of Infrared Spectra: A Practical Approach*, John Wiley & Sons, Inc., 2000.
28. R. M. Romano, C. O. Della-Vedova, and A. J. Downs, *J. Phys. Chem*., 2004, **A108**, 7180.
29. S. F. Sun, *Physical Chemistry of Macromolecules: Basic Principles and Issues*, John Wiley & Sons, Inc., 1994.
30. J. A. Barltrop, and J. D. Coyle, *Excited States in Organic Chemistry*, John Wiley & Sons, Ltd., 1975.
31. M. J. Frisch, G. W. Trucks, H. B. Schlegel, G. E. Scuseria, M. A. Robb, J. R. Cheeseman, J. A. Montgomery, Jr., T. Vreven, K. N. Kudin, J. C. Burant, J. M. Millam, S. S. Iyengar, J. Tomasi, V. Barone, B. Mennucci, M. Cossi, G. calmani, N. Rega, G. A. Petersson, H. Nakatsuji, M. Hada, M. Ehara, K. Toyota, R. ukuda, J. Hasegawa, M. Ishida, T. Nakajima, Y. Honda, O. Kitao, H. Nakai, M. Klene, X. Li, J.E. Knox, H. P. Hratchian, J. B. Cross, C. Adamo, J. Jaramillo, R.Gomperts, R. E. tratmann, O. Yazyev, A. J. Austin, R. Cammi, C. Pomelli, J. W. Ochterski, P.Y. Ayala, K. Morokuma, G. A. Voth, P. Salvador, J. J. Dannenberg, V. G. Zakrzewski, S. Dapprich, A. D. Daniels, M. C. Strain,O. Farkas, D. K. Malick, A.

D. Rabuck, K. Raghavachari, J. B. Foresman, J. V. Ortiz, Q. Cui, A. G. Baboul, S. Clifford, J. Cioslowski, B. B. Stefanov, G. Liu, A. Liashenko, P. Piskorz, I. Komaromi, R. L. Martin, D. J. Fox, T. Keith, M. A. Al-Laham, C. Y. Peng, A. Nanayakkara, M. Challacombe, P. M. W. Gill, B. Johnson, W. Chen, M. W. Wong, C. Gonzalez, and J. A. Pople, *Gaussian 03, Revision B. 01*, Gaussian, Inc., Pittsburgh PA, 2003.

32. T. Augustine, S. M. Vithiya, V. Ramkumar and C. C. Kanakam, *Acta Cryst*., 2008, **E64**, 2080.
33. J. D. Yoneda, P. R. Seidl, K. Z. Leal, M. G. Campos and R. Rittner**,** *J. Mol. Struct. (Theochem),* 2006, **767,** 29.
34. A. Katrusiak et al., *Acta Cryst.,*, 1987, **C43**, 105.
35. J. Mutanyatta, B. G. Matapa, D. D. Shushu, and B. M. Abegaz, *Phytochemistry*, 2003, **62**, 797.
36. S. F. Tayyari et al, *Spectrochimica Acta*, 2007, **A66**, 628.
37. D. Meksuriyen, G. A. Cordell, N. Ruangrungsi, and P. Tantivatana, *J. Nat. Prod.*, 1987, **50**, 1118.
38. D. D. McPherson, G. A. Cordell, D. D. Soejarto, J. M. Pezzuto, and H. H. S. Fong, *Phytochemistry*, 1983, **22**, 2837.
39. D. S. Kim, N. Baek, S. Angoh, K. Y. Jung, and I. S. Lee, *Phytochemistry*, 1997, **46**, 177.
40. C. Fuke, J. Yamahara, T. Shimokawa, J. Kinjo, T. Tomimatsu, and T. Nohara, *Phytochemistry*, 1985, **24**, 2403.
41. J. Mutanyatta, B. G. Matapa, D.D. Shushu and B. M. Abegaz, *Phytochemistry*, 2003, **62**, 801.
42. D. Dolphin, and A. Wick, *Tabulation of Infrared Spectral Data*, John Wiley & Sons, Inc., 1977.
43. A. Silayo, B. T. Ngadjui, B. M. Abegaz, *Phytochemistry*, 1999, **52**, 947.